IEICE TRANS. COMMUN., VOL.E97–B, NO.10 OCTOBER 2014

PAPER

Quantification and Verification of Whole-Body-Average SARs in Small Animals Exposed to Electromagnetic Fields inside Reverberation Chamber

Jingjing SHI[†a)], **Jerdvisanop CHAKAROTHAI**[††b)], ***Members***, **Jianqing WANG**[†c)], ***Fellow***, **Kanako WAKE**[††], **Soichi WATANABE**[††], ***Members***, ***and*** **Osamu FUJIWARA**[†], ***Fellow***

SUMMARY This paper aims to achieve a high-quality exposure level quantification of whole-body average-specific absorption rates (WBA-SARs) for small animals in a medium-size reverberation chamber (RC). A two-step method, which incorporates the finite-difference time-domain (FDTD) numerical solutions with electric field measurements in an RC-type exposure system, has been used as an evaluation method to determine the whole-body exposure level in small animals. However, there is little data that quantitatively demonstrate the validity and accuracy of this method in an RC up to now. In order to clarify the validity of the two-step method, we compare the physical quantities in terms of electric field strength and WBA-SARs by using a direct numerical assessment method known as the method of moments (MoM) with ten homogenous gel phantoms placed in an RC with 2 GHz exposure. The comparison results show that the relative errors between the two-step method and the MoM approach are approximately below 10%, which reveals the validity and usefulness of the two-step technique. Finally, we perform a dosimetric analysis of the WBA-SARs for anatomical mouse models with the two-step method and determine the input power related to our developed RC-exposure system to achieve a target exposure level in small animals.

key words: *specific absorption rate (SAR), reverberation-chamber (RC), exposure system, finite-difference time-domain (FDTD) method, method of moments (MoM)*

1. Introduction

Biological effects of electromagnetic fields (EMF) exposure have been raising public concerns with the rapid increase of wireless base stations and cellphone utilization. The safety standards for human exposure to radio frequency EMF have been promulgated in various national or international guidelines worldwide to ensure the protection of humans against any effect of EMF exposure [1]. A whole-body-average-specific absorption rate (WBA-SAR), or a temporally and spatially averaged power deposited over the whole body mass, is used as the physical quantity of exposure assessment in view of the long-term base station EMF exposure. According to the International Commission on Non-Ionizing Radiation Protection guidelines (ICNIRP), the WBA-SAR is restricted to 0.4 W/kg for occupational people, 0.08 W/kg for general public with a reduction rate of 5 [2]. Meanwhile, the World Health Organization (WHO) made strong recommendations on promoting the animal experiments and expert dosimetric supports for experimental studies in this domain [3]. Studies using human volunteers provide valuable insight into the short term physiological effects of EMF exposure on humans, however, animal studies give opportunities to investigate the possible effects of long term EMF exposure, which cannot be conducted with human volunteers. As a result, in order to investigate the potential adverse biological effects, an animal experiment with high-quality exposure level quantification is indispensable in order to link a biological effect to the exposure level. This requires that the WBA-SAR is kept at the designed level with a variability as small as possible in the small animal experiment.

A reverberation chamber (RC) has been widely used for immunity testing measurements in electromagnetic compatibility (EMC) field. To simulate the electromagnetic (EM) environment inside an RC, different numerical approaches such as the finite-difference time-domain (FDTD) method, finite element method (FEM), method of moment (MoM), have been used [4]–[6]. In the last several years, RC-type exposure systems were developed for non-restrained small animal exposure experiments and have been adopted worldwide [7]–[9].

Due to the difficulty in WBA-SAR measurements, the SAR values are mainly calculated using numerical techniques. The most popular one is the FDTD method, which solves the Maxwell equations in a differential form. By linking the FDTD-calculated average SAR values to the electric field strength measured in an RC, an incident power related to the RC can be determined and regulated to achieve a requisite exposure level as done in [9]. We define the above method as "two-step method", in which the electric field measurement and FDTD simulation are combined together to determine the WBA-SAR for small animals in the RC. The two-step method consists of the following steps,

Step 1: measure the average electric field strength inside the RC with small animals,
Step 2: calculate the SAR with numerical anatomical models by the FDTD simulation.

Manuscript received February 21, 2014.
Manuscript revised June 16, 2014.

[†]The authors are with Nagoya Institute of Technology, Nagoya-shi, 466-8555 Japan.
[††]The authors are with National Institute of Information and Communication Technology, Koganei-shi, 184-0015 Japan.
a) E-mail: shi@nitech.ac.jp
b) E-mail: jerd@nict.go.jp
c) E-mail: wang@nitech.ac.jp

DOI: 10.1587/transcom.E97.B.2184

This two-step method avoids direct modeling of the RC in the FDTD simulation in which the convergence of the calculated fields is difficult. In the second step of the two-step method, the FDTD simulation for SAR calculation is on the basis of plane wave superposition from various incident directions with random phases, which simulates an ideal EM environment with uniform field distribution in the RC [10].

In reality, however, the EM fields inside an RC strongly depend on the RC size, stirrers and antenna, so that the fields distributed in the RC may not be perfectly uniform. As a direct assessment method of the WBA-SAR in a non-ideal medium-size RC, we have proposed employing the MoM, and its validity has been clarified experimentally [6]. A major disadvantage in the direct MoM approach is that the MoM is difficult to give the SARs for inhomogeneous biological bodies such as anatomical mouse models in the RC, especially local SARs in a specific region such as brain, heart, etc.. A biological study usually requires not only the WBA-SAR data but also the SAR in a specific region to clarify possible biological effects of EMF exposure. The two-step method can provide a solution to satisfy these requirements. On account of this point, the two-step method should be more appropriate in the exposure level quantification of animal experiments with RCs. A problem with regard to the two-step method is that the validity and accuracy of this technique have not been well investigated so far.

Thus, in this study, we first dedicate ourselves to verify the two-step method in our developed RC-type exposure system by comparing physical quantities (electric field strength and WBA-SAR) derived from the two-step method and the direct MoM approach. Then, we perform a dosimetric analysis with the two-step method and determine the input power required in order to achieve a target exposure level in small animals. This paper is organized as follows. In Sect. 2, we describe our developed RC-type exposure system, and the measurement of average electric field strength and the FDTD numerical solutions of the WBA-SAR in the two-step method. The direct MoM approach for comparison is also described. In Sect. 3, we show our measured and simulated results in the two-step method for homogeneous biological-equivalent phantoms in comparison with those of the direct MoM approach to clarify the validity of the two-step method. After the validation of the two-step method, Sect. 4 gives the WBA-SAR quantification for inhomogeneous anatomical mouse models in the RC to link the antenna input power and electric field strength in our RC-type exposure system to the actual exposure level. Section 5 concludes this paper.

2. RC-Type Exposure System and Two-Step Method for SAR Quantification

On account of the good spatial uniformity of field distribution in an RC, the International Electrotechnical Commission employed it as a testing method in IEC 61000 – 4 – 21 for EM immunity, radiated emission and shielding-effectiveness measurements [11]. After that, worldwide research institutes began using this technique for exposure experiments to investigate biological effects of EM fields. Our developed medium-size RC consists of a rectangular enclosure and two stirrers, which are made of aluminum. There is a SMA connector on the RC roof, so that different antennas can be fixed through it easily. The dimensions of the RC are 1.2 m × 1.0 m × 0.8 m. Both two stirrers are installed almost vertically close to lateral wall and side wall respectively, and each of the stirrers has a size of 64 cm × 24 cm. The two stirrers can be rotated with different degrees by a connected controller to make the electric field distribution inside the RC statistically uniform. An air filter is also installed to supply fresh air for animals to relieve their stress caused by EM exposure.

As introduced in the previous section, the two-step method we employed in this study is composed of two steps. The first step is to measure the average electric field strength inside the RC, and the second step is to calculate the SARs with anatomically based numerical mouse models by FDTD simulation. In this section, we first describe the electric field measurement condition in the first step, and then the FDTD simulation for SAR calculation in the second step. Finally we verify the validity of the two-step method for WBA-SAR by comparison with the direct MoM approach result.

2.1 Step 1: Measurement of Electric Field Distribution

As the first step of the two step method to evaluate the WBA-SAR of biological bodies inside the RC, the average electric field strength should be measured in an actual RC exposure system with exposed biological bodies. The required electric field strength to produce a target SAR can be regulated by an antenna input power of the RC. Figure 1 shows a measurement system of the electric field distribution with homogeneous dielectric gel phantoms inside the RC. A helical antenna at 2 GHz was used to produce the EM fields inside the RC, and it was connected to a signal generator through a power meter with a 50 Ω coaxial cable. The antenna input power of the RC was obtained by the power meter and a

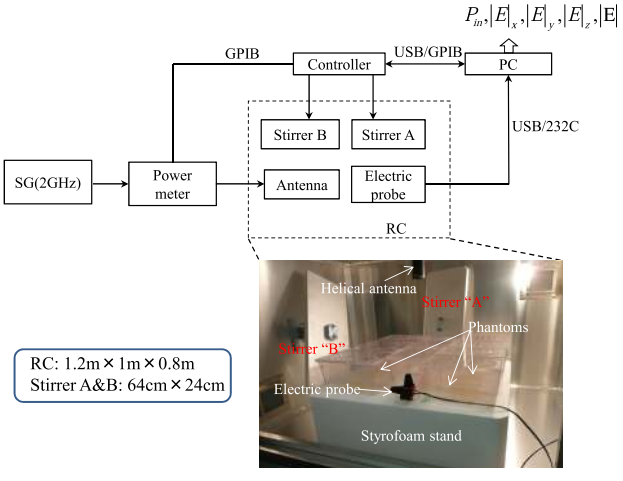

Fig. 1 Block diagram of electric field measurement system in RC.

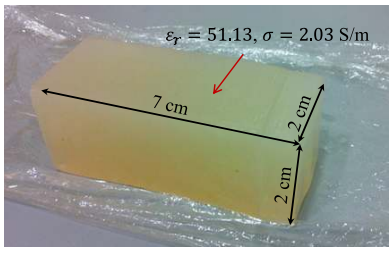

Fig. 2 Homogeneous gel phantom at 2 GHz.

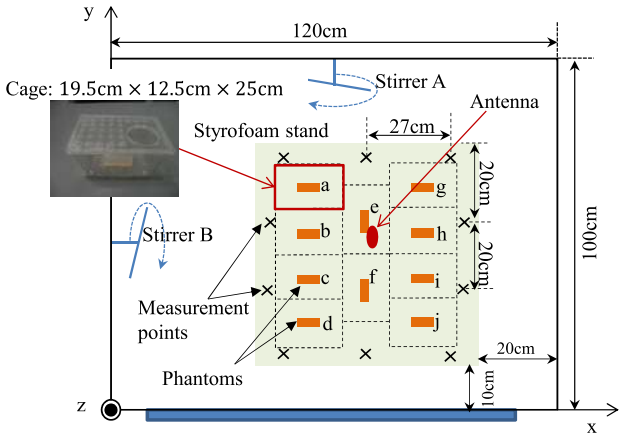

Fig. 3 Top view of the placement and measurement points inside the RC.

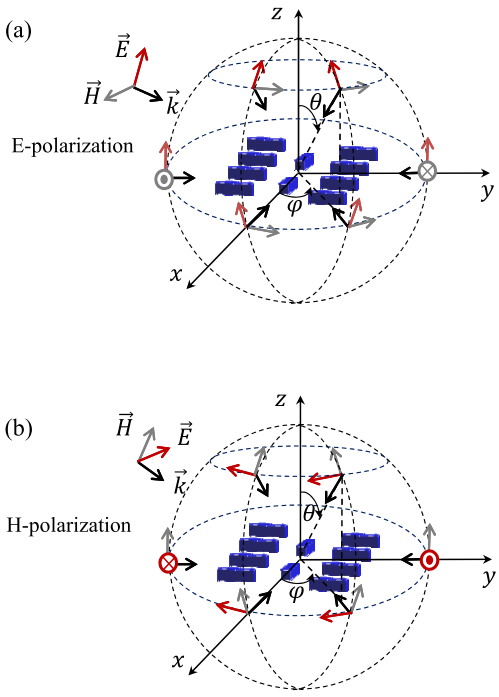

Fig. 4 EM plane-wave incidence in spherical form for simulating an ideal RC-type exposure with (a) E-polarization and (b) H-polarization.

three-axis electric field probe was used to record the temporal electric field strength of $|E_x|$, $|E_y|$, $|E_z|$ and $|E|$ in the RC. Stirrers "A" and "B" were controlled by a controller through a computer. We made both stirrers rotate counterclockwise from the same initial position at 0° by 5° angle step for stirrer "A" and, by 7.5° angle step for stirrer "B". If stirrer "A" rotates for 360°, then stirrer "B" should rotate for 540°. During one round rotation, the measurements took three minutes approximately. Figure 2 shows a homogeneous gel phantom, which had a rectangular shape with dimensions of 2 cm × 2 cm × 7 cm approximately. The relative permittivity ε_r, conductivity σ and density ρ of the phantom were 51.13, 2.03 S/m, and 1000 kg/m^3, respectively, at 2 GHz. In the measurements, the same ten gel phantoms were used. A styrene foam with dimensions of 60 cm × 60 cm × 25 cm was placed in the RC as a working stand, on which the ten gel phantoms, each one was placed in a plastic cage, were arranged with an equal spacing. The detailed specifications, placements, phantom labels, as well as the measurement locations of electric field strength are shown in Fig. 3.

2.2 Step 2: WBA-SAR Calculation with FDTD Method

In the second step of the two-step method, in order to simulate the same situation as in the RC, it assumes EM plane-waves irradiating from all directions with a constant electric field strength, since the exposure to the experimental animals in the RC could be considered as a far-field spherical irradiation under an ideal RC condition. Figure 4 shows EM plane-wave irradiations for ten dielectric phantom models with (a) E-polarization and (b) H-polarization. The incident direction of the EM plane-wave is defined by angles φ and θ. E-polarization irradiation is defined so as to have an electric field along the tangential direction of the longitude of the sphere, and a magnetic field along the tangential direction of the latitude of the sphere. H-polarization irradiation is defined so as to have a magnetic field along the tangential direction of the longitude of the sphere, and an electric field along the tangential direction of the latitude of the sphere. For complete simulation for an ideal RC, of course, all of the incident angle pairs should be taken into account to obtain the SAR values. According to [12], however, nine incident directions in each of the polarization irradiations are sufficient to obtain a convergent value for the WBA-SAR values. In fact, we investigated the WBA-SARs with three to nine incident directions for our mouse models. Based on the investigated results, the WBA-SAR of the mouse models may reach a steady state as long as the incident number is over than 5, since the relative error with five, six, seven or eight incident directions was below 3% compared to that with nine incident directions. As a result, we chose nine incident directions of EM plane-wave irradiation in order to obtain a more accurate WBA-SAR. In this study, we therefore employed a 40° interval of the angles of φ and θ at both the longitude and latitude directions, which results in 81 EM plane-wave irradiations with E-polarization and 81 EM plane-wave irradiations with H-polarization, respectively, and 162 EM plane-wave irradiations in total to calculate the WBA-SARs of the ten gel phantom models inside the RC. In the FDTD calculations, we used perfectly matched layers

(PML) as an absorbing boundary condition to avoid spurious reflections. The cell size was 1 mm × 1 mm × 1 mm, and the calculation lasts up to 8 periods of the sinusoidal waveform at 2 GHz until it reaches a steady state. As the exposure targets, ten lossy rectangular models had the same dielectric properties and arrangements as the gel phantoms in the experiment shown in Fig. 3. Each model also had a dimension of 2 cm × 2 cm × 7 cm and a weight of 30 g, which were approximately identical to those of the phantom in the measurement.

2.3 MoM Approach for Comparison

The MoM approach based on Poggio-Miller, Chang-Harrington, and Wu-Tsai (PMCHWT) formulation, provides a direct assessment for obtaining the WBA-SAR of lossy dielectric bodies placed inside the RC [6]. Different from the two-step method, this approach does not need the electric field measurement in an actual RC system. It simulates a real situation inside the RC by considering the coupling among the chamber, antenna, and exposed biological bodies, but suffers from the difficulty in analyzing inhomogeneous objects like anatomical numerical models. Here we used the MoM approach for comparison to verify the accuracy of the two-step method because the gel phantoms used in the electric field strength measurement were homogeneous.

In the MoM approach, the RC and the stirrers had the same dimensions as those of the real RC-type exposure system in Sect. 2. The helical antenna at 2 GHz was also used to produce the EM fields inside the RC. The parameters and placements of the rectangular homogeneous gel models were the same as those in measurement and FDTD simulation. Similar to the FDTD analysis in the two-step method, the cages were also neglected in the MoM approach due to their very low dielectric constants. In order to produce the EMF inside the RC, both stirrers "A" and "B" were set to elevate 5° with respect to z-axis and then rotate 15° in x-y plane as the initial state. The rotation steps were 15° and 22.5°, respectively for stirrers "A" and "B", and the total steps were 24, which results in one round rotation of 360° for stirrer "A" and 540° rotation for stirrer "B". The validation of this approach and the corresponding analysis parameters setting for the RC has been confirmed experimentally in [6].

3. Results and Discussion

3.1 Electric Field Verification

As shown in Fig. 1 and Fig. 3, the electric field strength was measured with a three-axis electric field probe at ten locations which surrounded the ten dielectric phantoms when the stirrers were rotating. The antenna input power was measured with a power meter to be from 1.7 mW to 2.89 mW when the stirrers were rotating, and the average input power was calculated as 2.45 mW. The average electric field strength was obtained during one round of the stirrers rotating at each measurement point.

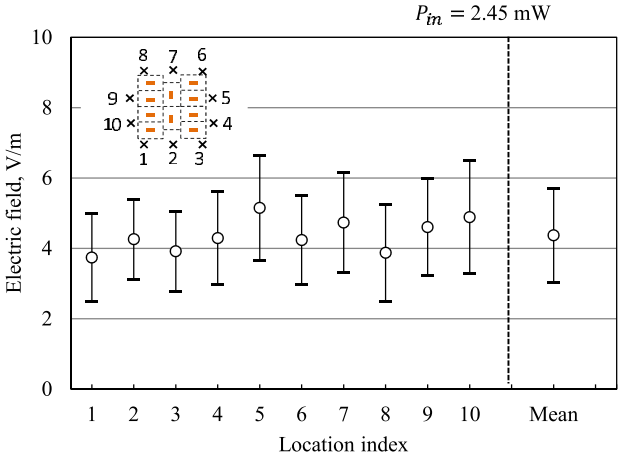

Fig. 5 Measured average electric field strength and standard deviations at the measurement points in the RC.

Figure 5 shows the temporally averaged electric field strength and standard deviation at each measurement point. The standard deviation was indicated as bars. It can be seen that the temporally averaged electric field strength for all the measurement points ranges from 3.74 V/m to 4.89 V/m, with the standard deviation from 1.13 V/m to 1.6 V/m. By using the temporally averaged electric field strength at each measurement point, we furthermore obtained the spatially averaged one for all the measurement points. The mean values of the electric field strength and standard deviation were 4.39 V/m and 1.34 V/m, respectively. This result indicates to what extent the electric field in our RC is uniformly distributed, and the obtained mean electric field strength will be used in the second step for SAR quantification.

Moreover, in Fig. 6, the statistical distributions of the normalized temporally measured electric field strength in x, y, and z directions were found to follow Rayleigh distribution, since they fit the theoretical characteristics inside the RC. The normalized electric field distribution derived from the MoM approach was also plotted for comparison. It can be observed that both the measured and MoM-calculated electric field strength data are in accordance with the theoretical Rayleigh distribution. As a result, it is concluded that the average electric field strength of 4.39 V/m can be produced inside the RC when the average input power of the helical antenna is 2.45 mW. Based on this finding, we can take the temporally and spatially averaged electric field strength as the plane-wave incident electric field strength in the second step of the two-step method for determining the WBA-SAR with the FDTD method. On the other hand, with the MoM approach, an average electric field strength of 5.2 V/m was obtained when the average input power was 2.75 mW.

The relationship between the spatial-average of the squared value of the electric field strength $\langle |E|^2 \rangle$ and the antenna input power P_{in} can be expressed as

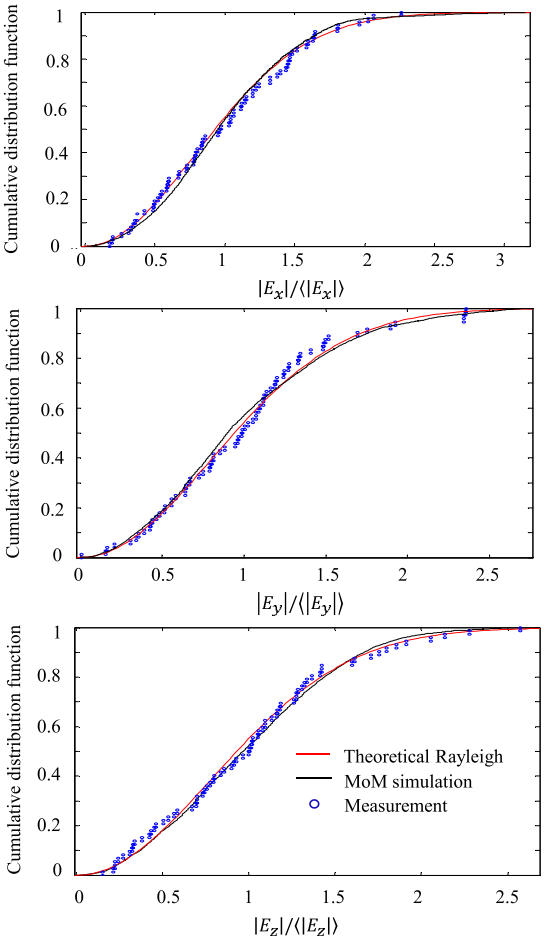

Fig. 6 Electric field distributions in the RC.

$$\langle|E|^2\rangle = K\eta P_{in} \tag{1}$$

where K and η indicate a radiation coefficient and intrinsic impedance in the RC, respectively. It should be noted that in our RC $\langle|E|^2\rangle$ is found equal to $\langle|E|\rangle^2$ within a difference of 1%. We therefore use the expression $\langle|E|\rangle$ for $\sqrt{\langle|E|^2\rangle}$ hereafter. When the stirrers in the reverberation chamber are well stirred, the EM field in the reverberation chamber can be represented by using a superposition of finite uniform plane-waves [10]. Since the wave impedance of a plane-wave in free space is 377 Ω, the intrinsic impedance in the reverberation chamber of 377 Ω should be a reasonable approximation. Under this assumption, we calculated the radiation coefficient K_{Meas} in the measurement as 20.9 m^{-2} and K_{MoM} in the MoM analysis as 26.1 m^{-2}. If we normalize the average input power P_{in} to 1 W, the average electric field strength produced inside the RC should be $\langle|E|_{Meas}\rangle$ = 88.8 V/m for the measurement and $\langle|E|_{MoM}\rangle$ = 99.2 V/m for the MoM, respectively. The relative error of electric field strength $\langle|E|_{Meas}\rangle$ to $|E|_{MoM}$ was approximately 10.5%. It should be noted that the cages existed in the experiment were not considered in the MoM analysis. So the corresponding losses in the cages may result in somewhat smaller electric field in the RC in comparison with the MoM analysis.

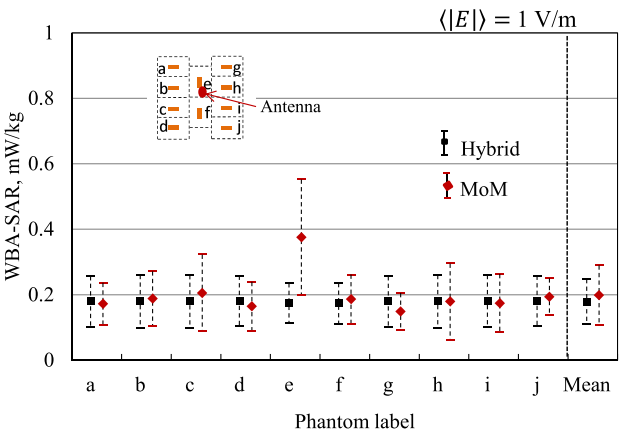

Fig. 7 WBA-SAR of each phantom placed in the RC with the two-step method and MoM approach.

3.2 WBA-SAR Verification

The mean WBA-SAR in this study is defined as the average value of the individual WBA-SAR in each dielectric gel phantom. Generally, SAR is given by

$$\mathrm{SAR} = \frac{\sigma|E|^2_{internal}}{\rho} \tag{2}$$

where $|E|_{internal}$ is the root mean square value of the internal electric field strength in the phantom, σ is the conductivity and ρ is the density. A target exposure level of WBA-SAR is determined by the squared value of average electric field strength $\langle|E|^2\rangle$, and $\langle|E|^2\rangle$ is proportional to the antenna input power P_{in}. In the two-step method, after measuring the averge electric field strength $\langle|E|_{Meas}\rangle$ inside the RC in the first step, the FDTD method was used to calculate the WBA-SAR and SAR distribution in the phantoms. By contrast, in the MoM approach, the electric field strength $\langle|E|_{MoM}\rangle$ and SAR distribution are calculated directly with the MoM.

Figure 7 shows the obtained average and standard deviation of WBA-SAR of each phantom with the two-step method and the MoM approach. The WBA-SAR variation was due to the rotation of the two stirrers. The mean WBA-SAR was the statistical mean of the WBA-SARs of the ten phantoms. For comparison, the average electric field strength in both the two approaches was normalized to 1 V/m. As a result, the mean WBA-SARs were $\mathrm{WBA\text{-}SAR}_{Two-step}$ = 0.18 mW/kg and $\mathrm{WBA\text{-}SAR}_{MoM}$ = 0.20 mW/kg, and the standard deviations were found to be 0.07 mW/kg in the two-step method and 0.09 mW/kg in the MoM approach, respectively. The relative error of the mean WBA-SAR between these two approaches was 10%. It should be noted that a higher WBA-SAR value was observed at phantom "e" in the MoM approach. This is because that phantom "e" was placed just beneath the antenna so that a direct path of the EM wave existed between this phantom and the antenna, which pro-

Table 1 Verification of two-step method with MoM approach.

(a) Average electric field strength (V/m) for P_{in} = 1 W

$\langle \|E\|_{Meas} \rangle$	$\langle \|E\|_{MoM} \rangle$	Relative error
88.8	99.2	10.5 %

(b) WBA-SAR (mW/kg) for $\langle |E| \rangle$ = 1 V/m

$\text{WBA-SAR}_{Two-step}$	WBA-SAR_{MoM}	Relative error
0.18	0.20	10 %

(c) Required average electric field strength (V/m) for WBA-SAR = 4 W/kg

$\langle \|E\|_{Two-step} \rangle$	$\langle \|E\|_{MoM} \rangle$	Relative error
149.5	143.0	4.5 %

duced a stronger exposure level. For the phantom "f", however, it was not placed just beneath the antenna. If excluding the special case of phantom "e", we can find that the WBA-SAR varies in a very narrow range from 0.15 mW/kg to 0.20 mW/kg. Consequently, the mean WBA-SAR would reduce to 0.18 mW/kg, which perfectly matched the two-step result. In the two-step method, the mean WBA-SAR of each phantom was found to be almost flat at 0.18 mW/kg due to the assumption of ideal RC.

Besides the comparison of WBA-SARs for a normalized average electric field strength, we also derived the required electric field strength $\langle |E|_{req} \rangle$ with the two approaches for obtaining a target exposure level WBA-SAR_{target} (4 W/kg) in the following way. Since WBA-SAR is proportional to $\langle |E|^2 \rangle \rightleftharpoons \langle |E| \rangle^2$, $\langle |E|_{req} \rangle$ is simply obtained from

$$\left\langle |E|_{req} \right\rangle = \sqrt{\frac{\text{WBA-SAR}_{target}}{\text{WBA-SAR}\big|_{\langle |E| \rangle = 1\ \text{V/m}}}}. \tag{3}$$

It was found from Eq. (3) that the required electric field strengths are 149.5 V/m in the two-step method and 143.0 V/m in the MoM approach. The relative error was derived as 4.5%. The above investigated results are summarized and tabulated in Table 1 to make the comparisons clear.

On the basis of our above investigations, the WBA-SARs derived from the two-step method agree well with the direct MoM approach results, which demonstrate the validity and usefulness of the two-step method for determining the WBA-SAR inside our developed RC.

4. Exposure Level Quantification for Anatomical Mouse Models

In the previous section, the two-step method which combines the FDTD numerical solution with the measured electric field strength to determine the exposure level of biological bodies in our developed RC, has been verified by means of a direct MoM approach, and its validity has been clarified with high accuracy in comparison with the MoM numerical results. In view of the difficulty in analyzing an anatomical mouse model by the MoM, in this section we employed the two-step method to perform a dosimetric analysis in the RC-type exposure system for actual small animals. Instead of the homogeneous dielectric lossy phantom

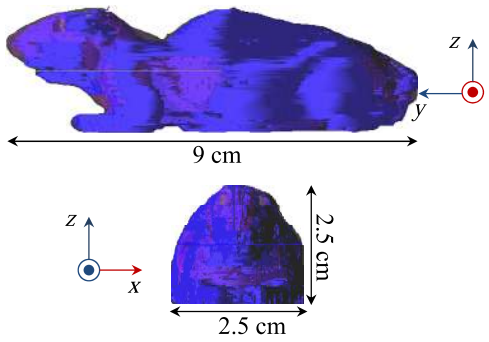

Fig. 8 Anatomical mouse model.

Table 2 Dielectric constants of anatomical mouse model.

Tissue type	Relative permittivity ε_r	Conductivity σ (S/m)
Skin	41.1	1.3
Fat	5.3	0.086
Muscle	53.3	1.5
Liver	43.8	1.4
Lung	35	1.1
Eyeball	53.3	1.7
Brain	43.2	1.3
Skull	15.4	0.5
Bowel	55.1	2.3
Stomach	62.9	1.8

model in the previous section, we employed an anatomical mouse model developed from magnetic resonance imaging data to derive the WBA-SAR in the RC. As can be seen in Fig. 8, our employed mouse model was developed by National Institute of Information and Communications Technology, Japan. It was composed of ten tissue types including skin, fat, muscle, liver, lung, eyeball, brain, skull, bowel, stomach with 1 mm resolution. Its maximum dimensions were 2.5 cm × 2.5 cm × 9 cm, and its weight was 25 g. The dielectric constants at 2 GHz for the biological tissues of the mouse model are tabulated in Table 2. With the same arrangements as that in previous sections, we obtained the WBA-SARs for the ten mouse models with the two-step method.

As can be seen in Fig. 9, the WBA-SAR was found to be 0.24 mW/kg with a variation in a narrow range between 0.22 mW/kg and 0.25 mW/kg. These results were derived with the average electric field strength $\langle |E| \rangle$ = 1 V/m. Moreover, the standard deviation of the WBA-SARs was found to be 0.06 mW/kg. Since the weight of the mouse model is 5 g lighter than that of the lossy phantom model in Sect. 2.2, the WBA-SAR values were somewhat higher than those in Fig. 7.

As a result, under the assumption that the ratio of the power deposited in the gel phantoms to the loss in the metal walls of the RC does not change with the antenna input power, when a target exposure level is given for the mice, a required input power $P_{in,req}$ or a required spatial-average electric field strength $\langle |E|_{req} \rangle$ related to our RC-type exposure system can be derived as

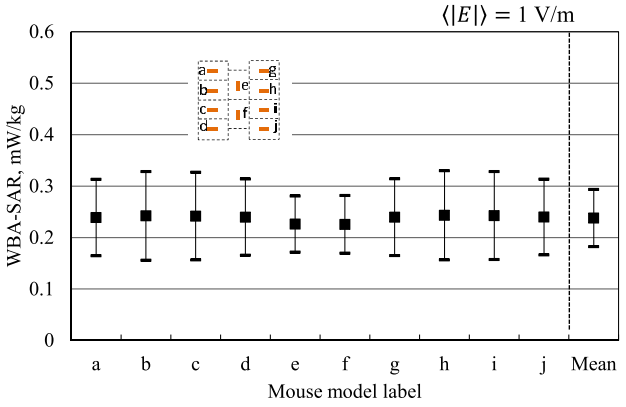

Fig. 9 WBA-SAR of each mouse model placed in the RC.

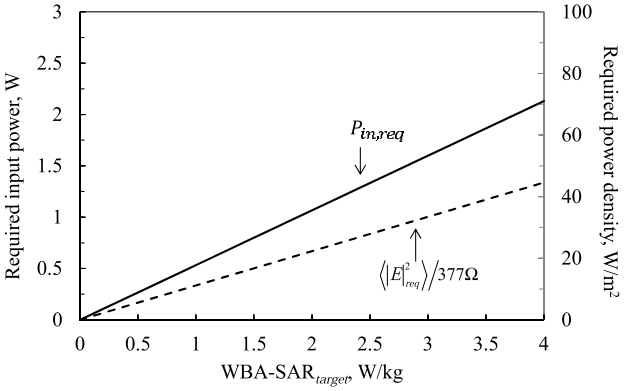

Fig. 10 Required input power and spatial-average power density versus WBA-SAR$_{target}$ for mice.

$$P_{in,req} = \frac{\langle|E|^2_{req}\rangle}{K\eta} \tag{4}$$

$$= \frac{\langle|E|^2_{req}\rangle}{\langle|E|^2_{req}\rangle\big|_{P_{in}=1\,\mathrm{W}}} \tag{5}$$

$$= \frac{\mathrm{WBA\text{-}SAR}_{target}}{\langle|E|^2_{req}\rangle\big|_{P_{in}=1\,\mathrm{W}} \times \mathrm{WBA\text{-}SAR}\big|_{\langle|E|\rangle=1\,\mathrm{V/m}}}, \tag{6}$$

which is based on the proportional relationship in Eqs. (1) and (3). Here, $\langle|E|^2_{req}\rangle|_{P_{in}=1\,\mathrm{W}}$ indicates the spatial-average of the squared value of electric field strength produced in the RC when giving 1 W antenna input power, and $\mathrm{WBA\text{-}SAR}|_{\langle|E|\rangle=1\,\mathrm{V/m}}$ indicates the WBA-SAR value derived from FDTD calculations with 1 V/m plane-wave incident electric field strength. By using the measured electric field strength in Sect. 3, we derived the relationship of required antenna input power, as well as required spatial-average electric field strength to achieve a WBA-SAR$_{target}$ with our develop RC-type exposure system, which is shown in Fig. 10. As can be seen in the figure, in order to achieve a WBA-SAR$_{target}$ of 4 W/kg, an antenna input power of 2.1 W should be required, and the corresponding required power density (= $\langle|E|^2_{req}\rangle/377\,\Omega$) is 44.6 W/m^2. If the WBA-SAR$_{target}$ decreases to 0.4 W/kg, the required input power and required power density will be proportionally reduced to 0.21 W and 4.46 W/m^2, respectively.

5. Conclusions

In this study, the validity of a two-step method, which combines electric field measurement with the FDTD solution to determine the WBA-SAR of small animals in an RC-type exposure system, has been verified with the direct MoM approach. Its accuracy in terms of relative errors in percentage to the MoM approach has been clarified to be approximately below 10% for the electric field strength and WBA-SAR in our developed medium-size RC. This result represents the first quantitative confirmation of the validity of the two-step method, although it has been used as a dosimetric tool in many RC-type exposure systems. On account of the good accuracy of the two-step method, we have applied it to the exposure level quantification in an exposure experiment for mice with our developed RC-type exposure system. As a result, in order to realize a mean WBA-SAR in the mice of 4 W/kg (or 0.4 W/kg) in the RC-type exposure system at 2 GHz, the antenna input power should be 2.1 W (or 0.21 W).

A future subject of this study is to apply this approach to higher frequencies.

Acknowledgment

This study was supported by the Ministry of Internal Affairs and Communications Japan.

References

[1] J.C. Lin, "Safety standard for human exposure to radio frequency radiation and their biological rationale," IEEE Microw. Mag., vol.4, pp.22–26, 2012.
[2] International Commission on Non-ionizing Radiation Protection, "Guidelines for limiting exposure to time-varying electric, magnetic, and electromagenic fields (up to 300 GHz)," Health Physics, vol.75, no.4, pp.494–522, 1998.
[3] "2006 WHO Research Agenda for Radio Frequency Fields," WHO, Geneva, Switzerland, 2006.
[4] F. Moglie and A.P. Pastore, "FDTD analysis of plane wave superposition to simulate susceptibility tests in reverberation chambers," IEEE Trans. Electromagn. Compat., vol.48, no.1, pp.195–202, 2006.
[5] C.F. Bunting, "Two dimensional finite element analysis of reverberation chambers; The inclusion of a source and additional aspects of analysis," Proc. IEEE Internation. Symp. on EMC, pp.219–224, Seattle, USA, Aug. 1999.
[6] J. Chakarothai, J. Wang, O. Fujiwara, K. Wake, and S. Watanabe, "Dosimetry of a reverberation chamber for whole-body exposure of small animals," IEEE Trans. Microw. Theory Tech., vol.61, no.9, pp.3435–3445, Sept. 2013.
[7] M. Capstick, N. Kuster, S. Kuhn, V. Berdinas-Torres, J. Ladbury, G. Koepke, D. McCormick, J. Gauger, and R. Melnick, "A radio frequency radiation reverberation chamber exposure system for rodents," Proc. 29th URSI Gen. Assembly, Art. ID A07.4, 2008.
[8] P.F. Biagi, L. Castellana, T. Maggipinto, G. Maggipinto, T. Ligonzo,

L. Schiavulli, and D. Loiacono, "A reverberation chamber to investigate the possible effects of in vivo exposure of rats to 1.8 GHz electromagnetic fields: A preliminary study," Progress in Electromagnetics Research, vol.94, pp.133–152, 2009.
[9] T. Wu, A. Hadjem, M.-F. Wong, A. Gati, O. Picon, and J. Wiart, "Whole-body new-born and young rats' exposure assessment in a reverberating chamber operating at 2.4 GHz," Physics in Medicine and Biology, vol.55, pp.1619–1630, 2010.
[10] D.A. Hill, "Plane wave integral representation for fields in reverberation chambers," IEEE Trans. Electromagn. Compat., vol.40, no.3, pp.209–217, 1998.
[11] IEC 61000-4-21 — Electromagnetic Compatibility (EMC) — Part 4-21: Testing and Measurement Techniques — Reverberation Chamber Test Methods, CISPR/A and IEC SC77B, IEC International Standard, Aug. 2003.
[12] J. Wang, T. Suzuki, O. Fujiwara, and K. Harima, "Measurement and validation of GHz-band whole-body average SAR in a human volunteer using average SAR in a human volunteer using reverberation chamber," Physics in Medicine and Biology, vol.57, pp.7893–7903, 2012.

Jingjing Shi received the B.E. degree from Shenyang University of Chemical Technology, Shenyang, China, in 2007, and the M.E. and D.E. degrees from Nagoya Institute of Technology, Nagoya, Japan, in 2010 and 2013, respectively. She is currently at Nagoya Institute of Technology as a Postdoctal Research Associate. Her research interests involve biomedical communications in wireless communication networks and biomedical EMC.

Jerdvisanop Chakarothai received his B.E. degree in electrical and electronic engineering from Akita University, Akita, Japan, in 2003, and his M.E. and D.E. degrees from Tohoku University, Sendai, Japan, in 2005 and 2010, respectively, both in electrical and communication engineering. He was a Research Associate at Tohoku University from 2010, prior to joining the Nagoya Institute of Technology, Nagoya, Japan, in 2011. He was a Research Associate at Tokyo Metropolitan University in 2013. He is currently with the National Institute of Information and Communications Technology, Tokyo, Japan. His research interests include computational electromagnetics (CEM) for biomedical communications and electromagnetic compatibility. Dr. Chakarothai is a member of the Institute of Electronics, Information and Communication Engineers, and a member of IEEE.

Jianqing Wang received the B.E. degree in electronic engineering from Beijing Institute of Technology, Beijing, China, in 1984, and the M.E. and D.E. degrees in electrical and communication engineering from Tohoku University, Sendai, Japan, in 1988 and 1991, respectively. He was a Research Associate at Tohoku University and a Senior Engineer at Sophia Systems Co., Ltd., prior to joining Nagoya Institute of Technology, Nagoya, Japan, in 1997, where he is currently a Professor. His research interests include biomedical communications and electromagnetic compatibility.

Kanako Wake received the B.E., M.E., and D.E. degrees in electrical engineering from Tokyo Metropolitan University, Tokyo, Japan, in 1995, 1997, and 2000, respectively. She is currently with the National Institute of Information and Communications Technology, Tokyo, Japan, where she is involved in research on biomedical EM compatibility. Dr. Wake is a member of the Institute of Electronics, Information and Communication Engineers (IEICE), Japan, the Institute of Electrical Engineers, Japan, and the Bioelectromagnetics Society. She was the recipient of the 1999 International Scientific Radio Union Young Scientist Award.

Soichi Watanabe received the B.E., M.E., and D.E. degrees in electrical engineering from Tokyo Metropolitan University, Tokyo, Japan, in 1991, 1993, and 1996, respectively. He is currently with the National Institute of Information and Communications Technology, Tokyo, Japan. His main research interest includes biomedical EM compatibility. Dr. Watanabe is a member of the Institute of Electronics, Information and Communication Engineers (IEICE), Japan, the Institute of Electrical Engineers, Japan, and the Bioelectromagnetics Society. From 2004 to 2012, he was a member of the Standing Committee III on Physics and Engineering, International Commission on Non-Ionizing Radiation Protection (ICNIRP). He is a member of the main commission of ICNIRP since 2012. He was the recipient of the 1996 Young Scientist Award of the International Scientific Radio Union, the 1997 Best Paper Award of the IEICE, and the 2004 Best Paper Award (The Roberts Prize) of Physics in Medicine and Biology.

Osamu Fujiwara received the B.E. degree in electronic engineering from the Nagoya Institute of Technology, Nagoya, Japan, in 1971, and the M.E. and D.E. degrees from Nagoya University, Nagoya, Japan, in 1973 and 1980, respectively, both in electrical engineering. From 1973 to 1976, he was with the Central Research Laboratory, Hitachi Ltd., Kokubunji, Japan, where he was engaged in research and development of system packaging designs for computers. From 1980 to 1984, he was with the Department of Electrical Engineering, Nagoya University, as a Research Associate, and from 1984 to 1985, as an Assistant Professor. In 1985, he joined the Nagoya Institute of Technology, as an Associate Professor. In 1993, he became a Professor with the Graduate School of Engineering, Nagoya Institute of Technology. In 2012, he retired and became an Emeritus Professor with the National University Corporation, Nagoya Institute of Technology. His research interests include measurement and control of EM interference due to discharge, bioelectromagnetics, and other related areas of EM compatibility. Dr. Fujiwara is a Fellow of the Institute of Electronics,Information and Communication Engineers (IEICE), Japan, and the Institute of Electrical Engineers, Japan (IEEJ). He is a member of the Bioelectromagnetic Society.